FRACTURE OF SOLID WOOD: A REVIEW OF STRUCTURE AND PROPERTIES AT DIFFERENT LENGTH SCALES

Michael P. C. Conrad

Graduate Research Assistant
Metals and Materials Engineering

Gregory D. Smith†

Assistant Professor
Wood Science

and

Göran Fernlund

Assistant Professor
Metals and Materials Engineering
University of British Columbia
Vancouver, BC Canada V6T 1Z4

ABSTRACT

This paper presents a review of the fracture literature of solid wood. The review is not exhaustive and is focused on the structure and properties of wood at different length scales. Fracture of wood has been examined in all pure modes as well as mixed-Mode I and II and all directions—radial, tangential, and longitudinal. The literature has been studied at a variety of levels from molecular through cellular and growth ring to macroscopic. The major conclusions are that fracture toughness perpendicular to the grain is greater than that parallel to the grain and Mode II is greater than Mode I, within a given species. Also, fracture toughness increases with increasing density and strain rate. Defects typically reduce the strength and fracture toughness, with edge defects having a greater effect. Finally, the fracture toughness of solid wood reaches a maximum between 6 to 8% moisture content. The paper discusses how these macroscopic observations are related to the chemical composition and micro/meso-structure of wood.

Keywords: Fracture mechanics, fracture morphology, solid wood, molecular structure, cellular structure.

INTRODUCTION

Fracture of solid wood can be examined on a variety of levels from molecular through cellular to macroscopic. An understanding of the mechanism of fracture at each level will give greater insight into the fracture of solid wood in general. Numerous authors have applied fracture mechanics to solid wood as a means of understanding the failure and predicting the strength of wooden structural members, with review articles written by Patton-Mallory and Cramer (1987) and Barrett (1981). It is typically assumed that wood behaves as a brittle solid, which is valid if the moisture content of the sample is sufficiently low. Wood is a natural material with inherent variability, and the associated physical and mechanical properties have coefficients of variation on the order of 20 to 25%. This variability leads to a wide range of quoted fracture toughness values even within a given species, thus creating difficulties in using these values for design purposes. In practice, the modulus of elasticity and the compressive strength perpendicular to the grain are based on average values, whereas

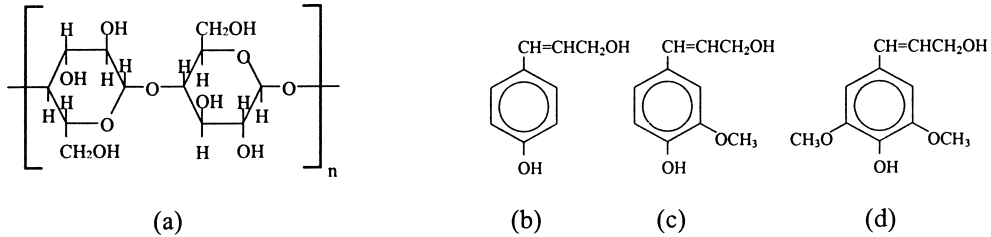† Member of SWST and corresponding author.

FIG. 1.   Molecular components of wood: repeat unit of cellulose—(a) cellobiose molecule (Nikitin 1966); monomers of lignin—(b) coniferyl alcohol, (c) sinapyl alcohol, and (d) *p*-coumarly alcohol (Lin and Lebo 1995).

all other properties use the values for the fifth percentile. The present review is focused on the structure and fracture properties at different length scales in an attempt to explain, or at least indicate, the relationship between wood structure at different length scales and macroscopic fracture properties.

In studying fracture mechanics of solids, three pure modes of crack propagation are typically examined. In addition, mixed-mode fracture, which involves a combination of two to three of the modes, is experienced. The three pure modes of fracture are described below.

Mode I: Opening or tensile mode, where the crack surfaces move directly apart.

Mode II: Sliding or in-plane shear mode, where the crack surfaces slide across one another in the direction perpendicular to the leading edge of the crack.

Mode III: Tearing or antiplane shear mode, where the crack surfaces move parallel to the leading edge of the crack.

Wood is a highly anisotropic material and these fracture modes are further divided by the three principal axes of anisotropy: radial (R), tangential (T), and longitudinal (L). A figure showing these directions is available from the Forest Product Society (1999), but is not reproduced here for brevity. The plane and direction of crack propagation are identified by a pair of letters. The first denotes the direction normal to the crack surface and the second the direction of crack growth. Fracture of wood can be simplified if the specimen is taken a sufficient distance from the tree center such that the curvature of the growth rings can be ignored. The specimen then behaves as an orthotropic material.

MOLECULAR SCALE

At the molecular level, wood consists of cellulose and lignin and other organic molecules such as hemicelluloses and uronic acids. Cellulose is a semi-crystalline polysaccharide based on 1,4 linked β-D-glucose molecules (Fig. 1a). The molecular weight (both number-average, $\bar{M}_n$, and weight-average, $\bar{M}_w$) and degree of polymerization (DP) of cellulose are difficult to obtain; however, evidence suggests that in higher plants the DP is 3500 to 7000 or higher based on the cellobiose repeat unit (Richmond 1991). Higher plants are cellulose-producing organisms that have conducting tissues. This includes plants that flower or produce cones, ferns, and others that are classified in the kingdom Plantae. The cellulose chains coalesce to form ordered, crystalline microfibrils that have high strength and stiffness in the longitudinal direction.

Lignin is considered an amorphous polymer that is based on the following monomers: Figs. 1b, c, and d. Because of the difficulty in isolating lignin from wood without degradation, the actual molecular weight of lignin is unknown. However, the $\bar{M}_w$ of softwood milled wood lignin is estimated at 20,000, with lower values reported for hardwoods. The polydispersity of lignin is also high ($\bar{M}_w/\bar{M}_n = 2.5$)
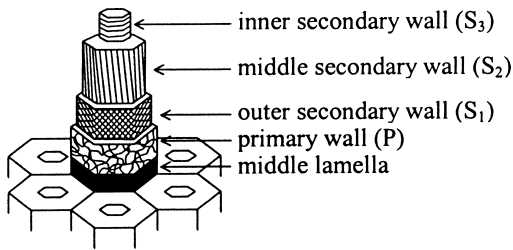
FIG. 2. Organization of the cell-wall layers and middle lamella. Adapted from Nikitin (1966).

compared with cellulose, indicating that it is a mixture of long and short molecules. The lower molecular weight and greater polydispersity of lignin lead to a lower fracture toughness than for cellulose.
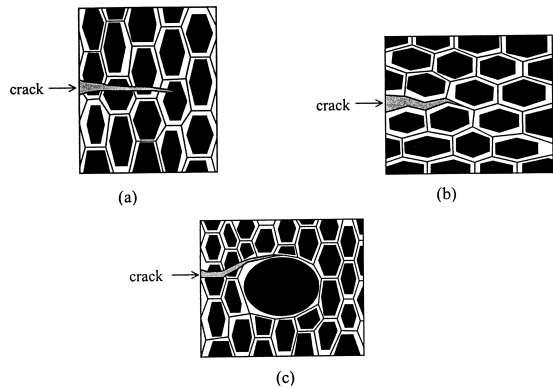

FIG. 3. Schematic of various crack paths in wood: (a) crack advance by cell fracture (intracellular fracture), (b) crack advance by cell separation (intercellular fracture), and (c) crack arrest at a vessel showing a crack splitting the wall of a vessel (crack deflection). Adapted from Gibson and Ashby (1988).

CELLULAR SCALE

At the cellular level, wood can be considered a fiber-reinforced polymer composite of cellulose microfibrils in a lignin matrix. The cell wall consists of four discrete layers (Nikitin 1966) where the orientation of the cellulose microfibrils varies from 0° to 90° to the longitudinal axis of the fiber; this is shown schematically in Fig. 2. The primary wall, P, is an irregular network of microfibrils with a lignin content of less than 50%. In addition, the cellulose chains within the primary wall microfibrils have a low DP, approximately 250, as compared with a DP of 3500 to 7000 for the cellulose found in the secondary wall. The microfibrils of the outer secondary wall, S_1, form two overlapping spirals resulting in a structure similar to a ±45 layer in a polymer composite. The middle secondary wall, S_2, forms the majority of the cell wall and consists of concentric layers of microfibrils oriented almost parallel to the fiber axis. Finally, the inner secondary wall, S_3, consists of microfibrils that lie nearly perpendicular to the fiber orientation. In total, the secondary wall of the cell contains 10 to 12% lignin. The cells are held together in a honeycomb fashion by the middle lamella, which consists of approximately 70% lignin distributed isotropically.

Since the majority of the cell-wall material is found in the S_2 layer, the strength of wood is greater in the longitudinal direction compared with the radial and tangential directions. Also, the secondary wall consists of approximately 80% of the total cellulose, and it has greater fracture toughness than the primary wall and middle lamella.

Moving towards the macroscopic scale, solid wood can be viewed as a honeycomb network of cells cemented together by the middle lamella. This leads to the two major fracture paths found in wood (Boatright and Garrett 1983; Gibson and Ashby 1988), cell fracture and cell separation (DeBaise 1972). The first is through cell fracture or intracellular fracture as shown in Fig. 3a. The type of fracture that occurs is determined to a large extent by the wood density. For convenience, the density of a wood is often given as the ratio of wood density, ρ, to that of the cell-wall material, ρ_s, which is typically 1500 kg/m^3. Cell fracture is generally found in low-density ($\rho/\rho_s < 0.2$) woods and the earlywood of higher density woods and is the typical failure mode in the RT, RL, LR, and LT directions.

Cell separation or intercellular fracture is shown in Fig. 3b. During cell separation, the crack propagates through the middle lamella and primary cell wall leaving the secondary

wall intact. This occurs in higher density woods ($\rho/\rho_s > 0.2$) along with some cell fracture. Gibson and Ashby (1988) found that propagation in the TR direction is through cell separation. In addition, a crack running at an angle between the RT and TR directions will tend to deviate toward the TR direction adopting the cell separation mode of fracture.

Cell fracture has higher fracture toughness than cell separation. This is shown by the greater fracture toughness of the RT, RL, LR, and LT directions over the TR and TL directions and the preference of the TR direction for a crack running at an angle between the RT and TR directions. The difference can be explained by the relative proportions of cellulose and lignin as well as the type of cellulose found in the various cellular layers. Since cellulose has higher fracture toughness than lignin and is predominantly found in the secondary cell wall, it is reasonable to assume that cell fracture, which occurs through fracture of the secondary cell wall, will have greater fracture toughness than cell separation. In addition, the cellulose in the primary cell wall has a significantly lower DP as compared with the cellulose in the secondary cell wall and exhibits lower fracture toughness.

Vessels affect the fracture path by acting as crack arrestors as shown in Fig. 3c. The crack path tends to deviate towards a vessel and either enter it or run partly around the edge of the channel and stop (Gibson and Ashby 1988). These are examples of extrinsic toughening mechanisms: crack-tip blunting and crack deflection, respectively.

With increasing temperature and moisture content, more viscoelastic deformation occurs, and there is a shift from cell fracture to cell separation. Also, this reduces the extent and frequency of unstable crack extension that typically occurs in the case of cell fracture as compared with slow crack growth that occurs in the case of cell separation (DeBaise 1972).

GROWTH RING SCALE

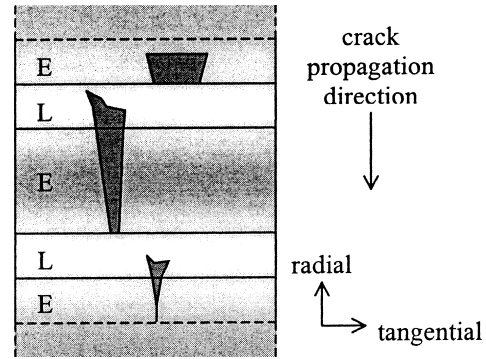As a tree grows over the course of a year, cells are added to the tree in two distinct lay-

FIG. 4. Schematic of crack propagating in the TR direction. E = earlywood, L = latewood. Adapted from Thuvander and Berglund (2000).

ers. Earlywood, grown during the spring, consists of large-diameter, thin-walled cells. Latewood, deposited later in the growing season, consists of smaller diameter cells with thicker cell walls. The repeated layering of the early and latewood produces the pattern known as growth rings. The difference in cellular structure of the earlywood and latewood leads to variations in density and stiffness, which further explain the difference in fracture toughness for the various directions. Thuvander et al. (2000a, b; Thuvander and Berglund 2000) demonstrate the increased fracture toughness of the TR direction over the TL direction. The crack propagates in the cell separation mode at the level of individual cells, and a stick-slip mechanism of crack growth was found at the growth ring scale due to the alternating stiff (latewood) and flexible (earlywood) layers. As well, crack propagation typically occurs through the formation of secondary cracks that are displaced tangentially from the primary crack where the latewood acts as a crack arrestor, shown schematically in Fig. 4. Further inactive secondary cracks are also found well away from the primary crack. Since energy is required to form the new surface area of the inactive secondary cracks, they contribute to the fracture toughness of wood.

The difference in stiffness between early and latewood also causes inclined cracks to deviate to the TR direction (Thuvander and

Berglund 2000). Inclined cracks are propagated by both cell fracture and cell separation with the latter mechanism being dominant. Upon reaching the latewood, the crack is arrested, and a secondary crack is initiated in the radial direction at a weak point in the latewood. As above, this secondary crack is displaced tangentially from the original, i.e., horizontally in Fig. 4.

<center>MACROSCOPIC SCALE</center>

While the knowledge gained in examining the fracture of wood at the molecular and cellular level is important, the majority of applications are on the macroscopic scale. Thus, the majority of researchers concentrate on this level. However, many of the effects seen at the macroscopic scale can be explained by phenomena at the molecular and cellular level. The literature on the macroscopic fracture toughness of wood can be divided into the three principal modes of crack propagation: Mode I, Mode II, and Mode III as well as mixed-mode fracture and studies on fracture strength.

Mode I fracture toughness

Mode I, or the opening mode of fracture, is considered the most important mode in engineering failures. However, wood often exhibits a significant component of Mode II fracture. Mode I fracture toughness is the most easily measured of the three modes; thus the majority of the literature concentrates on this property.

A summary of some of the work to date on the fracture of solid wood is listed in Table 1 by fracture specimen geometry, direction of crack growth, species, and effect examined.

The possible directions of a Mode I fracture toughness test can be grouped into those where the crack is propagating perpendicular to the grain (LR and LT) and those parallel to the grain (RL, TL, RT, TR). The Mode I fracture toughness of wood perpendicular to the grain is approximately one order of magnitude greater than the fracture toughness in the other directions as shown in Table 2. This is due to

the crack propagating by cell fracture rather than cell separation. Cell fracture also leads to the slightly higher value of fracture toughness for the RL direction over the TL direction. It should be noted that cracks tend to propagate parallel to the grain even if the starter crack is originally in the LR or LT direction.

A variety of fracture toughness specimens have been used to characterize the Mode I fracture toughness of wood. Wood properties are inherently variable, and no major difference in Mode I fracture toughness due to specimen geometry has been reported. The ASTM Standard E399-90: Standard Test Methods for Plane-Strain Fracture Toughness of Metallic Materials (1994) is typically applied to wood. However, Bostrom (1990) recommends against using the CT specimen for measuring the Mode I fracture toughness of solid wood due to difficulties in determining when the crack begins propagating.

The Mode I fracture toughness of solid wood is affected by strain rate, moisture content, density, defects, and thickness. The effect of strain rate has been examined by various authors (Blicblau and Cook 1986; Ewing and Williams 1979b; Johnson 1973; Mai 1975; Mindess et al. 1975a, b; Nadeau et al. 1982; Schniewind and Pozniak 1971). With the exception of Mai (1975), they concluded that the fracture toughness of wood increases with strain rate. This is due to subcritical crack growth that causes delayed failure of wood (also known as the duration-of-load effect where the fracture toughness of wood specimens decreases as a function of time). At lower strain rates, there is sufficient time for cracks to reach the critical size, at which point the test specimen fails catastrophically. At higher strain rates, less time is available for crack growth, and the fracture toughness of these samples is higher than for specimens strained more slowly.

Studies on moisture content have examined wood from oven-dry to green (Ewing and Williams 1979a; Johnson 1973; Kretschmann et al. 1990; Mai 1975; Mindess 1977; Petterson and Bodig 1983; Sobue et al. 1985), although

TABLE 1. *Mode I fracture toughness specimen geometries, directions, species, and effect examined.*

Specimen geometry	Direction						
	RL	TL	RT	TR	LR	LT	N/A
Compact Tension (CT)	P*: (1)***	P: (2, 3, 4) S: (3) *MC***: (2) ρ: (2)		P: (4, 5, 6)			P, S, *T*: (7)
Notched Four Point Bend	DF, *SR*: (8)				HF, *D, MC*: (9) *AT*, ρ: (10)	HF, *MC*: (9) U, *D*: (11) DF, *SR*: (12) *AT*, ρ: (10)	
Double Torsion	DF, *SR*: (13)						
Single Edge Notch (SEN)	DF, *MC*: (14)	DF: (14, 15) B: (16) P: (17) *MC*: (14, 17) *D*: (15, 17) *T*: (16)	DF, *MC*: (14) S: (18)	DF: (14, 19) P: (19) B: (20) S: (18) *MC*: (14) *SR*: (19)	DF, *MC*: (14) P, *D*: (21)	DF, *MC*: (14) P, *D*: (21)	
Tapered Cleavage	P, *SR*: (22)						
Double Cantilever Beam (DCB)	S, *SR, MC*: (23) P: (24)	DF, *D*: (25) B: (16, 26) P: (24) C, S, H, L: (26) *MC*: (26) DF: (25)		DF, *D*: (25)			
Double Edge Notch (DEN)		DF: (25)		DF: (19, 25) P: (19)			
Center Notch (CN)	P, DF, C, M, Bi, O, La, *SR, MC*: (27)	P: (27) DF: (25, 27) P, C, M, Bi, O, La: (27) *SR*: (25, 27) *MC*: (27)		DF, *SR*: (25)	P: (21)	P: (21)	
Wedge	S: (28)				S: (28)		
Unknown							ρ: (29, 30)

* Species: T = Australian Timber, B = beech, Bi = birch, C = cedar, DF = Douglas-fir, H = hemlock, HF = hem-fir, L = larch, La = lauan, M = maple, O = oak, P = pine, S = spruce, U = unknown.

** Effects: *D* = defects, *MC* = moisture content, ρ = density, *SR* = strain rate, *T* = thickness.

*** Authors: 1 = Bostrom 1990; 2 = Kretschmann et al. 1990; 3 = Riipola and Fonselius 1992; 4 = Thuvander and Berglund 2000; 5 = Thuvander et al. 2000b; 6 = Thuvander et al. 2000a; 7 = Wright and Fonselius 1986; 8 = Mindess et al. 1975; 9 = Mindess 1977; 10 = Leicester 1947a; 11 = Boatright and Garrett 1979; 12 = Nadeau et al. 1982; 13 = Mindess et al. 1975b; 14 = Schniewind and Centeno 1973; 15 = Schniewind and Lyon 1973; 16 = Triboulot et al. 1984; 17 = Ewing and Williams 1979a; 18 = Atack et al., 1961; 19 = Blicblau and Cook 1986; 20 = Sobue et al. 1985; 21 = Pearson 1974; 22 = Ewing and Williams 1979b; 23 = Mai 1975; 24 = Valentin and Morlier 1982; 25 = Schniewind and Ponziak 1982; 26 = Petterson and Bodig 1983; 27 = Johnson 1973; 28 = Schachner et al. 2000; 29 = Gibson and Ashby 1988; 30 Leicester 1983.

TABLE 2. *Mode I fracture toughness of air-dry Douglas-fir. (Schniewind and Centeno 1973).*

Direction	K_{Ic} (MPa·m$^{1/2}$)
RL	0.41
TL	0.31
RT	0.35
TR	0.35
LR	2.69
LT	2.42

the moisture content is typically between 10 to 15% (Boatright and Garrett 1979; Ewing and Williams 1979b; Schniewind and Centeno 1973; Triboulot et al. 1984). Ewing and Williams (1979b) found that the fracture toughness of wood initially increases from an oven-dry condition reaching a maximum between 6 to 8%, and then decreases monotonically thereafter. This increase in Mode I fracture toughness with moisture content is due to increased viscoelastic behavior of the wood (Mindess 1977), leading to greater energy absorption through viscous deformation and an increased toughness. However, above the level of 6 to 8%, it appears the Mode I fracture toughness becomes constant or decreases slightly (Kretschmann et al. 1990). More recently, Kretschmann and Green (1996) found that the Mode I fracture toughness of Scots pine increased as the moisture content decreased from the green state to approximately 8%, where it reached a maximum, and decreased for lower moisture contents. The slight decrease in Mode I fracture toughness for moisture contents above 8% may be due to the ingress of water into the crystal structure of the cellulose microfibrils. This leads to a reduction in crystallinity and a subsequent reduction in fracture toughness (Nikitin 1966). For higher moisture content values, the validity of fracture mechanics becomes questionable due to increased plasticity during crack propagation. Evidence of plastic work during the fracture event was observed by Atack et al. (1961).

The reduction of Mode I fracture toughness at low moisture contents is due to the difference in shrinkage rate of the radial, tangential, and longitudinal directions. These lead to residual drying stresses (Ewing and Williams 1979a; Sobue et al. 1985) that produce radial cracks and a subsequent reduction in fracture toughness. Schniewind and Centeno (1973) varied the relative humidity between 35 and 87% with the humidity held at each value for 12 h and have shown that cyclic changes in humidity can significantly decrease the time to failure of solid wood.

The fracture toughness of wood increases with increasing density (Ashby et al. 1985; Gibson and Ashby 1988; Kretschmann et al. 1990; Leicester 1974a; Leicester 1983; Petterson and Bodig 1983), as shown in Fig. 5. It should also be noted that this is true for green wood (Petterson and Bodig 1983) where the validity of fracture mechanics is questionable. The following relationships between density and K_{Ic} have been postulated:

$$K_{Ic}{}^n = 20\left(\frac{\rho}{\rho_s}\right)^{3/2} \qquad (MPa·m^{1/2})$$

$$\text{Ashby et al (1985),} \qquad (1)$$

$$K_{Ic}{}^a = 1.81\left(\frac{\rho}{\rho_s}\right)^{3/2} \qquad (MPa·m^{1/2})$$

$$\text{Ashby et al (1985),} \qquad (2)$$

$$K_{Ic}{}^n = 0.0047\rho \qquad (MPa·m^{1/2})$$

$$\text{Leicester (1983),} \qquad (3)$$

$$K_{Ic}{}^a = 0.00063\rho \qquad (MPa·m^{1/2})$$

$$\text{Leicester (1983),} \qquad (4)$$

$$K_{Icg} = 0.00062(\rho)^{0.952} \quad (MPa·m^{1/2})$$

$$\text{Petterson and Bodig (1983),} \quad (5)$$

where $K_{Ic}{}^n$ = Mode I fracture toughness normal to the grain (LR, LT direction),

$K_{Ic}{}^a$ = Mode I fracture toughness along the grain (RL, TL, RT, TR direction),

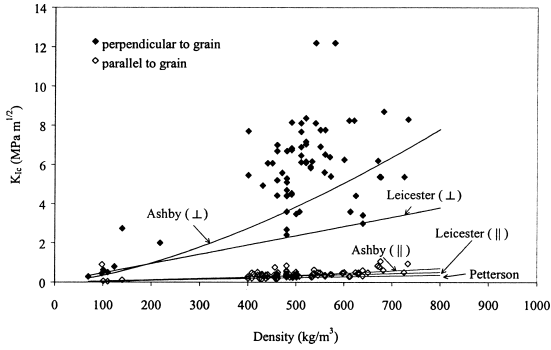K_{Icg} = Mode I fracture toughness

FIG. 5.   Effect of density on Mode I fracture toughness. Data obtained from Ashby et al. 1985; Bostrom 1990; Johnson 1973; Kretschmann et al. 1990; Lei and Wilson 1980; Mindess et al. 1975b; Nadeau et al. 1982; Patton-Mallory and Cramer 1987; Pearson 1974; Schniewind and Centeno 1973; Schniewind and Lyon 1973; Schniewind and Pozniak 1971; White and Green 1980.

along the grain for green wood,

ρ = wood density (kg/m^3, and
ρ_s = density of cell-wall material (1500 kg/m^3).

It should be noted that all of the relationships between fracture toughness and density shown in Eqs. (1) to (5) are the result of a least squares fit to a log-log plot of the data and are neither average nor 5th percentile values.

The model put forth by Leicester underestimates the effect of density on Mode I fracture toughness normal to the grain, whereas the model by Ashby agrees better with experimental data. However, the Ashby, Leicester, and Petterson and Bodig models fit well for fracture toughness along the grain. The increase in fracture toughness with density is due to the increase in the amount of wood as compared to voids in a given cross-section and is comparable with the effect of latewood on the crack path as reported by Thuvander and Berglund (2000).

Ewing and Williams (1979a), Wright and Fonselius (1986), and Triboulot et al. (1984) examined the effect of thickness on the Mode I fracture toughness. Ewing demonstrates the effect of moving from the plane stress regime to the plane strain regime as the fracture

toughness decreases to a plateau when the thickness is increased. Wright and Fonselius found that for pine, spruce, and spruce-laminated veneer lumber (LVL), a specimen thickness of 20 mm was sufficient to achieve plane strain conditions. Triboulot et al. (1984) also show that the necessary thickness for plane strain is on the order of 20 mm where 65% of the specimen is in a plane strain condition.

The defects studied include notches (Ewing and Williams 1979a; Mindess 1977; Schniewind and Pozniak 1971), checks (Schniewind and Lyon 1973; Schniewind and Pozniak 1971), and knots (Boatright and Garrett 1979; Pearson 1974). Ewing and Williams (1979a) states that the effect of changing notch depth (5 to 15 mm) and notch radius (from less than 5 to 300 μm) was inconclusive in the ranges studied. Schniewind and Pozniak (1971) found that Douglas-fir specimens with a notch length of either 0.14 in. or 0.16 in. failed away from the pre-existing notch tip. This confirms the existence of inherent flaws in Douglas-fir on the order of 0.15 in. Checks were found to reduce the fracture strength and toughness of solid wood to a greater degree then other defects when the wood is tested perpendicular to the grain (Schniewind and Lyon 1973). Checks are radial cracks formed due to differences in radial and longitudinal shrinkage upon drying and terminate in a sharp crack tip, whereas other defects studied such as resin streaks, pitch pockets, and pith are blunt. This difference in crack tip radius causes the greater reduction in fracture toughness by checks over other wood defects.

Mode II fracture toughness

While Mode I fracture is typically considered the driving force behind engineering failures in most materials, experience has shown that wood failure often has a significant Mode II component. Table 3 summarizes the literature on Mode II fracture toughness for the specimen geometries, directions, species, and effects that have been examined. The orthotropic directions that have been studied are RL

TABLE 3. *Mode II fracture toughness specimen geometries, directions, species, and effect examined.*

| | Direction | | | | | | |
Specimen geometry	RL	TL	RT	TR	LR	LT	N/A
End Notched Flexure (ENF)	DF*, *CL***: (1)***	DF, *CL*: (3)					P, S: (4)
	H, *CL*: (2)	H, *CL*: (2, 3)					*MC*, ρ: (5)
Center-Slit Beam (CSB)	DF, *CL*, ρ: (6)						
Compact Shear (CS)		P, DF, *MC*: (7)					
Compact Tension Shear (CTS)	P: (8)						
Center Notch Under Shear							Ba: (9)

* Species: Ba = balsa, DF = Douglas-fir, H = hemlock, P = pine, S = spruce.
** Effects: *CL* = crack length, *MC* = moisture content, ρ = density.
*** Authors: 1 = Murphy 1979a; 2 = Barrett and Foschi 1977a; 3 = Barrett and Foschi 1977b; 4 = Wright and Fonselius 1986; 5 = Fonselius and Riipola 1988; 6 = Murphy 1989; 7 = Cramer and Pugel 1987; 8 = Valentin and Caumes 1989; 9 = Wu 1967.

and TL. No literature on the other directions has been found—likely due to the difficulty of obtaining beams of significant length where the length is not parallel to the longitudinal direction.

The majority of the researchers (Barrett and Foschi 1977a, b; Cramer and Pugel 1987; Murphy 1989) have found that it is difficult to obtain values for pure Mode II failure due to the low Mode I fracture toughness parallel to the grain. Very little stress is required to precipitate failure in this direction and therefore, Mode I failure may occur away from the desired location (Cramer and Pugel 1987) or the specimen may fail earlier than predicted (Barrett and Foschi 1977b) for pure Mode II loading. Closing friction and minor changes in specimen geometry may also affect the calculated values for K_{II} and K_{IIc} leading to greater variability in these values compared with K_I and K_{Ic}. However, the absolute values for K_{IIc} are consistently greater than K_{Ic} for the corresponding direction. For example, Douglas-fir in the TL direction has a K_{Ic} of 0.36 MPa·m$^{1/2}$ (Schniewind and Centeno 1973) and a K_{IIc} of 1.56 MPa·m$^{1/2}$ (Cramer and Pugel 1987).

Varying the moisture content from 10 to 20% (Fonselius and Riipola 1988) appears to have little effect on Mode II fracture toughness, which agrees with the results for Mode I fracture toughness, although the range studied was small. More recently, Kretschmann and Green (1996) studied the Mode II fracture toughness of Scots pine and found that the Mode II fracture toughness increases steadily when drying from the green state, peaking at approximately 12% and decreasing for lower moisture contents. Cramer and Pugel (1987) found that a harsher drying history, which produces more and larger flaws within the sample, led to a decrease in K_{IIc}.

A similar relationship to that for Mode I exists between density and Mode II fracture toughness, as K_{IIc} also increases with increasing density (Fonselius and Riipola 1988; Leicester 1974a, 1983; Murphy 1989). This similarity between Modes I and II is also seen for varying crack lengths with an increase in crack length leading to an increase in the Mode II fracture toughness for end-notched flexure and center-slit beam specimens (Barrett and Foschi 1977a, b; Murphy 1979b, 1989).

Mixed-mode fracture toughness

Since pure Mode I or pure Mode II are rarely encountered in practice, a number of researchers have examined mixed mode fracture. Studies in mixed mode failure have given empirical mixed-mode failure criteria, based on knowledge of pure Mode I and II values, for use in design. The literature on mixed mode fracture toughness is summarized in Table 4.

The following empirical failure criterion (Eqs. 6 to 13) have been proposed for the onset of mixed-mode fracture:

TABLE 4. *Mixed Mode fracture toughness specimen geometries, directions, and species.*

Specimen geometry	Direction						
	RL	TL	RT	TR	LR	LT	N/A
Modified End-Notched Flexure (mENF)	BR*: (1)**						H: (2)
Compact Shear (CS)	P: (3)	P: (3)		P: (3)			
		S: (4)					
Compact Tension Shear (CTS)	P: (3)	P: (3)		P: (3)			
End-Notched Flexure (ENF)		DF, H: (5)					
Single Edge Notch (SEN)		S: (4)					
Center Notch (CN)		S: (4)					Ba (6)

* Species: Ba = balsa, BR = Baltic redwood, DF = Douglas-fir, H = hemlock, P = pine, S = spruce.
** Authors: 1 = Hunt and Croager 1982; 2 = Lum and Foschi 1988; 3 = Valentin and Caumes 1989; 4 = Mall et al. 1983; 5 = Barrett and Foschi 1977b; 6 = Wu 1967.

$$\frac{K_I}{K_{Ic}} = 1 \qquad (K_{II} \geq 0)$$

Mall et al. (1983)   (6)

$$\frac{K_I}{K_{Ic}} + \frac{K_{II}}{K_{IIc}} = 1$$

Leicester (1974b)   (7)

$$\frac{K_I}{K_{Ic}} + \alpha\left(\frac{K_{II}}{K_{IIc}}\right)^{\beta} = 1$$

Hunt and Croager (1982)   (8)

where $\alpha = 1.005$ and $\beta = 3.4$,

$$\frac{K_I}{K_{Ic}} + \left(\frac{K_{II}}{K_{IIc}}\right)^2 = 1$$

Leicester (1983) and Wu (1967)   (9)

$$\left(\frac{K_I}{K_{Ic}}\right)^2 + \frac{K_{II}}{K_{IIc}} = 1$$

Mall et al. (1983)   and   (10)

$$\left(\frac{K_I}{K_{Ic}}\right)^2 + \frac{K_{II}}{K_{IIc}} = 1$$

Mall et al. (1983).   (11)

The criterion that best predicts the mixed-mode failure is that postulated by Wu (1967), who studied balsa. The same failure criterion, Eq. (13), was also found to give the best correlation with experimental data in a later study by Mall et al. (1983), who examined spruce. The fact that a single mixed-mode failure criteria adequately describes the behavior of balsa and spruce may be coincidental; however, this failure criteria may describe the behavior of a wide variety of species. Further work is necessary to determine this.

Mode III fracture toughness

The final mode of fracture is Mode III: the tearing or antiplane shear mode. This has been examined by Murphy (1980) using a side-cracked cantilever beam of Sitka spruce in the RT direction obtaining a K_{IIIc} of 0.66 MPa·m$^{1/2}$.

This is comparable to Mode I or Mode II failure in the RL direction; however, due to differences in species between Mode I and Mode III, this comparison cannot be made at the present. For Mode II, the fracture toughness for spruce in the RL direction is approximately twice that of Mode III in the RT direction. Murphy found that for crack ratios (crack length/specimen width) below 0.15, the beam behaves as if it were composed of clear wood. The shear span also affects the Mode III fracture toughness; as the shear span (length vs. width) and hence the crack width increases, K_{IIIc} is reduced. It should be noted that Murphy's work was validated using built-up I-beams rather than solid wood beams with cracks or slits. Caution should be used when extrapolating these experimental results to solid wood specimens due to differences in the stress fields.

More recently, Erhart et al. (1999) developed a specimen and an experimental setup that allows testing in Mode I, Mode III, and

TABLE 5. *Specimen geometries, directions, species, and effect examined in the study of fracture strength.*

Specimen geometry	Direction	
	TL	N/A
Four Point Bend		DF*: (1, 2)***
		E: (3)
		H: (4, 5)
		Bm, C: (5)
		SR**: (2)
		D: (1, 2, 3)
		MC: (5)
Three Point Bend		DF: (1)
Tension	DF, D: (6)	

* Species: Bm = balsam, C = cedar, DF = Douglas-fir, E = eucalyptus.
** Effects: *D* = defects, *MC* = moisture content, *SR* = strain rate.
*** Authors: 1 = Murphy 1979a; 2 = Spencer 1979; 3 = Leicester 1973; 4 = Lum and Foschi 1988; 5 = Steida 1966; 6 = Cramer and Goodman 1983.

Mixed-mode I–III. They found that the fracture energy values were substantially greater for Mode III than for Mode I.

Fracture strength

Experiments on the fracture strength or failure load of wood, summarized in Table 5, demonstrate the applicability of fracture mechanics to the study of wood failure. Fracture mechanics predicts both the effect of defects such as notches and knots as well as the effect of moisture content.

Knots in wood significantly disturb the regular grain structure of wood, which in turn leads to changes in the fracture toughness. The effect, however, is unclear since the knot may increase K_{Ic} in some cases and decrease it in others. Boatright and Garrett (1979) found that the knot ratio, which is the ratio of the amount of specimen perimeter that is covered by knots to the entire specimen perimeter (Eq. 12) shown in Fig. 6, was the best indicator of the effect of knots on the fracture toughness of solid wood. The knot ratio, *KR,* depends on the position of the knot within the board and takes into account the increased effect of edge knots over face knots as well as its size. For example, the face knot shown on the left side of Fig. 6 only contributes the vertical length of the knot to the numerator of the knot ratio, whereas the edge knot shown on the right side
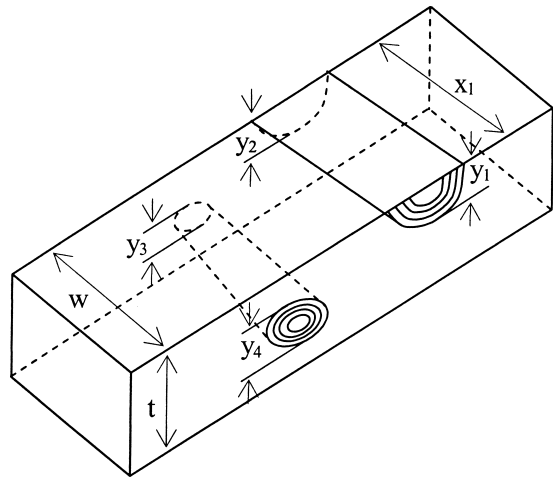

FIG. 6.   Diagram showing the values used in calculating the knot ratio, *KR.* Adapted from Boatright and Garrett (1979).

of the figure has the contributions of both the vertical and horizontal length of the knot. The strength of the specimen decreases with increasing knot ratio.

$$KR = \frac{\sum (x_i + y_i)}{2(w + t)}, \qquad (12)$$

where x_i = the length of the knot exposed to the surface of the board,

           y_i = the length of the vertical axis of the knot,

           w = the width of the board, and

           t = the thickness of the board.

Pearson (1974) modelled knots with equivalent cracks and found that if the crack length was taken to be the same as the knot dimensions, the fracture toughness was underestimated. This suggests that a knot cannot be modelled by a crack. Fracture mechanics confirms this as the maximum stress at the tip of an elliptical crack in an isotropic, elastic, infinite body is given by:

$$\frac{\sigma_{max}}{\sigma_a} = 1 + \frac{2a}{b}, \qquad (13)$$

where σ_{max} = maximum applied stress at the end of the major axis,

σ_a = applied stress applied normal to the major axis,

a = half major axis, and

b = half minor axis,

and shows that as the minor axis is reduced, i.e., the crack tip becomes sharper, the maximum stress at the end of the major axis increases. Since knots typically have a larger minor axis than a crack, an equivalent crack will underestimate the fracture toughness of a knot.

While the majority of researchers do not state the orthotropic direction studied, it is presumably either the RL or TL direction. As with Mode II fracture toughness, it is difficult to obtain sufficiently large specimens where the length is not parallel to the longitudinal direction.

Several researchers (Leicester 1973; Leicester and Poynter 1979; Stieda 1966; Lum and Foschi 1988) have studied the effect of notches on failure load, modulus of rupture (MOR), and stress intensity factor. Lum and Foschi (1988) have shown that for a rectangular end-notched flexure (rENF) specimen, the Mode I stress intensity factor increases with notch depth and notch length. It should be noted that this is not pure Mode I loading and therefore must be categorized as mixed-mode. Leicester (1973; Leicester and Poynter 1979) found that as the sharpness of the notch tip increases, the MOR and failure load of the specimen are reduced. This was also observed by Stieda (1966), who reported a similar effect for notch depth, which is an equivalent concept to crack length.

As with Mode I fracture, knots affect the failure load. Using finite element analysis, Cramer and Goodman (1983) show that edge knots lead to a greater stress concentration, defined as σ_{max}/σ_a, than face knots. This confirms the effect found by Pearson (1974) where the fracture strength of edge knots, modelled by an equivalent crack, was between 30 to 62% of the fracture strength for a similarly sized face knot.

Stieda (1966) examined the effect of moisture content on the failure mechanism. As the moisture content is increased to fiber saturation, the material behavior shifts from brittle to tough. This is similar to results for Mode I and Mode II fracture. Initial failure at the notch for dry material typically resulted in complete failure of the beam, as is the case for brittle materials. In contrast, initial failure in green material resulted in a small load drop followed by a subsequent increase in load, as the green specimens failed slowly by shear at the notch tip rather than sudden cross-grain failure as is the case for dry beams.

The effect of strain rate was examined by Spencer (1979), who found that bending strength increased with strain rate. The effect was more pronounced for samples with a greater initial strength, which likely have a smaller intrinsic flaw size. The mechanism for the increased bending strength at higher strain rates is likely the same as that for Mode I fracture toughness.

Energy methods and nonlinear fracture mechanics

The literature discussed above has mainly been using the concepts of linear elastic fracture mechanics (LEFM) and in particular the stress intensity factor (K) approach. LEFM requires that the material be linear elastic, or at least that any material nonlinearity be restricted to a small region in the vicinity of the crack tip (small scale yielding). If these conditions are met, K is a measure of the intensity of the stress and strain field in the crack tip region. Energy methods do not explicitly consider the local stresses and strains in the vicinity of the crack tip and are based on the concept of an energy balance between elastic energy in the system and the energy required to extend the crack. Energy methods can be used when the material behavior is linear elastic (LEFM), and they can be extended to cases when the material behavior is nonlinear (NLEFM). Compared to the LEFM literature, the NLEFM literature is limited. Although NLEFM is more cumbersome to apply, Gustafsson (1988) pointed out the NLEFM is more appropriate

in many applications where the condition of linearity is violated. Examples when NLEFM should be used are when there are creep effects, crack bridging behind the crack tip, and when a fracture process zone with damage and microcracks develops around the crack tip. Some notable work in the area has been done by Bostrom (1992) and Tan et al. (1995), who studied the softening of the process zone ahead of the crack tip, and Vasic and Smith (2002), who developed a crack bridging model for fracture of spruce. NLEFM and the understanding of how the fracture process zone develops in different species, modes of loading, and crack orientations are currently poorly understood. However, nonlinear techniques are required to understand and predict creep, R-curve behavior, and damage tolerance of large scale wood structures.

SUMMARY AND CONCLUSIONS

Review of the literature on the fracture of solid wood at different length scales shows that its behavior is dependent on the mode of loading (Mode I, Mode II, Mode III, and mixed-modes) and the direction of crack propagation (RL, TL, RT, TR, LR, and LT) because of anisotropy of the structure and properties of wood. To understand and interpret the macroscopic behavior of wood, fracture needs to be examined at all scales: molecular, cellular, growth ring, and macroscopic, with insight into the behavior at each level provided from the understanding of its behavior at the finer scale.

Thus, the major conclusions found on the macroscopic fracture of solid wood can be related to the behavior of wood at the lower levels. These major conclusions are that the fracture toughness perpendicular to the grain is approximately one order of magnitude greater than that parallel to the grain. Fracture perpendicular to the grain occurs by destruction of the cellulose microfibrils rather than simple cleavage leading to increased fracture toughness. Increasing fracture toughness with increasing density can also be related to the cel-

lular level, as the crack must pass through a greater amount of cellulose, which has a high fracture toughness, to propagate. Finally, fracture toughness increases with moisture content, reaching a maximum between 6 to 8%, and decreasing thereafter. This is due to a shift in fracture behavior from brittle to ductile. At higher moisture contents, the crystal structure of the microfibrils is disturbed by the increased water and hence fracture toughness is reduced.

Other conclusions are based on an understanding of fracture mechanics. Mode II fracture toughness is greater than Mode I for a given species as is the case with the majority of materials. Fracture toughness increases with increasing strain rate since the internal flaws do not have sufficient time to reach the critical length. Checks and other defects reduce the strength and fracture toughness of a specimen as they introduce flaws greater than those inherently found in the material. However, in the case of knots, there is the possibility of an increase in fracture toughness. Also, as with most materials, edge defects have a greater effect than face defects.

This review has shown that we can interpret and to some extent explain the macroscopic fracture behavior based on an understanding of the structure and properties at smaller length scales. However, currently we do not have sufficient understanding to directly and quantitatively relate chemical composition and micro/meso-structure to the microscopic and macroscopic fracture behavior of wood.

REFERENCES

AMERICAN SOCIETY FOR TESTING AND MATERIALS (ASTM). 1994. Standard test method for plane-strain fracture

toughness of metallic materials. Annual Book of ASTM Standards. E399-90, 03.01, 407–437.

ASHBY, M. F., K. E. EASTERLING, R. HARRYSON, AND S. K. MAITI. 1985. The fracture and toughness of woods. Proc. Royal Soc. London A A398:261–280.

ATACK, D., W. D. MAY, E. L. MORRIS, AND R. N. SPROULE. 1961. The energy of tensile and cleavage fracture of black spruce. TAPPI 44(8):555–567.

BARRETT, J. D. 1981. Fracture mechanics and the design of wood structures. Philo. Trans. Royal Soc. London 299:217–226.

———, AND R. O. FOSCHI. 1977a. Mode II stress-intensity factors for cracked wood beams. Eng. Fract. Mech. 9: 371–378.

———, AND ———. 1977b. Shear strength of uniformly loaded dimension lumber. Can. J. Civil Eng. 4:86–95.

BLICBLAU, A. S., AND D. J. COOK. 1986. Aspects of wood fracture toughness at various testing speeds. Civil Eng. Trans. 153–158.

BOATRIGHT, S. W. J., AND G. GARRETT. 1979. The effect of knots on the fracture strength of wood—I. A review of methods of assessment; II. A comparative study of methods of assessment, and comments on the application of fracture mechanics to structural timber. Holzforschung 3:68–77.

———, AND ———. 1983. The effect of microstructure and stress state on the fracture behaviour of wood. J. Mat. Sci. 18:2181–2199.

BOSTROM, L. 1990. The compact tension test used on wood—An analysis of a testing method. IUFRO S5.02—Timber Engineering.

———. 1992. Method for determination of the softening behaviour of wood and applicability of a non-linear fracture mechanics model. Lund University TVBM-1012, Lund, Sweden.

CRAMER, S. M., AND J. R. GOODMAN. 1983. Model for stress analysis and strength prediction of lumber. Wood Fiber Sci. 15(4):338–349.

———, AND A. D. PUGEL. 1987. Compact shear specimen for wood mode II fracture investigations. Int. J. Fracture 35:163–174.

DEBAISE, G. R. 1972. Morphology of wood shear fracture. J. Materials 7(4):568–572.

ERHART, R. J. A., S. E. STANZL-TSCHEGG, AND E. K. TSCHEGG. 1999. Mode III fracture energy of wood composites in comparison to solid wood. Wood Sci. Technol. 33:391–405.

EWING, P. D., AND J. D. WILLIAMS. 1979a. Thickness and moisture content effect in the fracture toughness of Scots pine. J. Mater. Sci. 14(May):2959–2966.

———, AND ———. 1979b. Slow crack growth in softwoods. ICM 3(August):293–298.

FONSELIUS, M., AND K. RIIPOLA. 1988. Mode II fracture toughness of wood effects of moisture and time. 1988 Int. Conf. Timber Eng. 2:601–609.

FOREST PRODUCTS SOCIETY. 1999. Mechanical properties Of wood. Pages 4–25 *in* Wood Handbook: Wood as an Engineered Material, Forest Products Society, Madison, WI.

GIBSON, L. J., AND M. F. ASHBY. 1988. Wood. Pages 278–315 *in* Cellular solids: Structure and properties. Pergamon Press, New York, NY.

GUSTAFSSON, P. J. 1988. A study of strength of notched beams. Proc., CIB-W18, Meeting 21. Vancouver, BC.

HUNT, D. G., AND W. P. CROAGER. 1982. Mode II fracture toughness of wood measured by a mixed-mode test method. J. Mat. Sci. Letters 1:77–79.

JOHNSON, J. A. 1973. Crack initiation in wood plates. Wood Science 6(2):151–158.

KRETSCHMANN, D. E., AND D. W. GREEN. 1996. Modeling moisture content-mechanical property relationships for clear southern pine. Wood Fiber Sci. 28(3):320–337.

———, ———, AND W. J. NELSON. 1990. The effect of moisture content on mode I fracture toughness in southern pine. IUFRO S5.02 Timber Eng. 274–303.

LEI, Y. K., AND J. B. WILSON. 1980. Fracture toughness of oriented flakeboard. Wood Science 12(3):154–161.

LEICESTER, R. H. 1973. Effect of size on the strength of structures. CSIRO Aust. Forest Prod. Lab., Div. Build. Res. Technol. Pap. No. 71:1–13.

———. 1974a. Fracture strength of wood. Pages 729–742 *in* Proc. First Australian Conference on Engineering Materials, University of New South Wales, Sydney, Australia.

———. 1974b. Applications of linear fracture mechanics in the design of timber structures. Proc. Australian Fracture Group Conference 23:156–164.

———. 1983. The fracture strength of wood. Workshop on timber engineering. Melbourne, Australia (11):1–24.

———, AND W. G. POYNTER. 1979. On the design strength of notched beams. 19th Forest Products Research Conference (Melbourne, Australia). 228–232.

LIN, S. Y., AND S. E. LEBO. 1995. Lignin. Kirk-Othmer Encyclopedia of Chemical Technology. 4th ed. Vol. 15. John Wiley & Sons, New York, NY. Pp. 268–289.

LUM, C., AND R. O. FOSCHI. 1988. Arbitrary V-notches in orthotropic plates. J. Eng. Mech. 114(4):638–655.

MAI, Y. W. 1975. On the velocity-dependent fracture toughness of wood. Wood Science 8(1):364–367.

MALL, S., J. F. MURPHY, AND J. E. SHOTTAFER. 1983. Criterion for mixed mode fracture in wood. J. Eng. Mech. 109(3):680–690.

MINDESS, S. 1977. The fracture of wood in tension parallel to the grain. Can. J. Civil Eng. 4:412–416.

———, J. S. NADEAU, AND J. D. BARRETT. 1975a. Effect of constant deformation rate on the strength perpendicular to the grain of Douglas-fir. Wood Science 8(4):262–266.

———, ———, AND ———. 1975b. Slow crack growth in Douglas-fir. Wood Science 8(1):389–396.

MURPHY, J. F. 1979a. Strength of wood beams with end splits. Research Paper FPL 3471-12. USDA Forest Serv., Forestry Prod. Lab.

———. 1979b. Using fracture mechanics to predict fail-

ure in notched wood beams. Pages 159–174 *in* Proc. First Int. Conf. on Wood Fracture. Forintek Canada Corp., Vancouver, BC, Canada.

———. 1980. Strength of wood beams with side cracks. IUFRO S5.02 Timber Engineering. 255–264.

———. 1989. Mode II wood test specimen: Beam with center slit. J. Testing Eval. 16(4):364–368.

NADEAU, J. S., R. BENNETT, AND E. R. FULLER, JR. 1982. An explanation for the rate-of-loading and the duration-of-load effects in wood in terms of fracture mechanics. J. Mater. Sci. 17:2831–2840.

NIKITIN, N. I. 1966. The chemistry of cellulose and wood. Israel Program for Scientific Translations, Jerusalem. 691 pp.

PATTON-MALLORY, M., AND S. M. CRAMER. 1987. Fracture mechanics: A tool for predicting wood component strength. Forest Prod. J. 37(7/8):39–47.

PEARSON, R. G. 1974. Application of fracture mechanics to the study of the tensile strength of structural lumber. Ho1zforschung 28:11–19.

PETTERSON, R. W., AND J. BODIG. 1983. Prediction of fracture toughness of conifers. Wood Fiber Sci. 15(4):302–316.

RICHMOND, P. A. 1991. Occurrence and functions of native cellulose. Pages 5–23 *in* C. H. Haigler, and P. J. Weimer, eds. Biosynthesis and biodegradation of cellulose. Marcel Dekker, Inc., New York, NY.

RIIPOLA, K., AND M. FONSELIUS. 1992. Determination of critical J-Integral for wood. J. Struct. Eng. 118(7):1741–1750.

SCHACHNER, H., A. REITERER, AND S. E. STANZL-TSCHEGG. 2000. Orthotropic fracture toughness of wood. J. Mater. Sci. Letters 19(20):1783–1785.

SCHNIEWIND, A. P., AND R. A. POZNIAK. 1971. On the fracture toughness of Douglas-fir wood. Eng. Fract. Mech. 2:223–233.

———, AND J. C. CENTENO. 1973. Fracture toughness and duration of load factor I. Six principal systems of crack propagation and the duration factor for cracks propagating parallel to grain. Wood Fiber 5(2):152–159.

———, AND D. E. LYON. 1973. A fracture mechanics ap-

proach to the tensile strength perpendicular to grain of dimension lumber. Wood Sci. Technol. 7:45–59.

SOBUE, N., D. BAJOLET, AND G. PLUVINAGE. 1985. Effect of drying stress on the fracture toughness of wood. Mokuzai Gakkaishi 31(7):528–531.

SPENCER, R. 1979. Rate of loading effect in bending for Douglas-fir lumber. Pages 259–279 *in* Proc. First Int. Conf. on Wood Fracture, Forintek, Canada, Corp., Vancouver, BC, Canada.

STIEDA, C. K. A. 1966. Stress concentrations around holes and notches and their effect on the strength of wood beams. J. Materials 1(3):560–582.

TAN, D.M., S.E. STAZL-TSCHEGG, AND E.K. TSCHEGG. 1995. Models of wood fracture in Mode I and Mode II. Holz. Roh- Weskst. 53:159–164.

THUVANDER, F., AND L. A. BERGLUND. 2000. In situ observations of fracture mechanisms for radial cracks in wood. J. Mater. Sci. 35(24):6277–6283.

———, L. O. JERNKVIST, AND J. GUNNARS. 2000a. Influence of repetitive stiffness variation on crack growth behaviour in wood. J. Mater. Sci. 35(24):6259–6266.

———, M. SJODAHL, AND L. A. BERGLUND. 2000b. Measurements of crack tip strain field in wood at the scale of growth rings. J. Mater. Sci. 35(24):6267–6275.

TRIBOULOT, P., P. JODIN, AND G. PLUVINAGE. 1984. Validity of fracture mechanics concepts applied to wood by finite element calculation. Wood Sci. Technol. 18:51–58.

VALENTIN, G., AND P. CAUMES. 1989. Crack propagation in mixed mode in wood: A new specimen. Wood Sci. Technol. 23:43–53.

VALENTIN, G., AND P. MORLIER. 1982. A criterion of crack propagation in timber. Materiaux et Constructions 15(88):291–298.

VASIC, S., AND I. SMITH. 2002. Bridging model for fracture of spruce. Eng. Fract. Mech. 69:745–760.

WHITE, M. S., AND D. W. GREEN. 1980. Effect of substrate on the fracture toughness of wood-adhesive bonds. Wood Science 12(3):149–153.

WRIGHT, K., AND M. FONSELIUS. 1986. Fracture mechanics testing of wood methods for mode I and mode II. CIB-WI8/19. 764–765.

WU, E. M. 1967. Application of fracture mechanics to anisotropic plates. J. Appl. Mech. 12:967–974.